Acta Cryst. (1982). B**38**, 140–149

The Charge Density in Imidazole by X-ray Diffraction at 103 and 293 K

BY JOEL EPSTEIN*

Chemistry Department, Carnegie–Mellon University, Pittsburgh, PA 15213, *USA*

AND JOHN R. RUBLE AND B. M. CRAVEN†

Department of Crystallography, University of Pittsburgh, Pittsburgh, PA 15260, *USA*

(*Received* 26 *January* 1981; *accepted* 18 *May* 1981)

Abstract

The static charge density has been determined for imidazole, based on X-ray (Mo $K\alpha$) intensity data [1892 reflections with $F_o > 6\sigma(F)$ and $\sin\theta/\lambda < 1{\cdot}3$ Å^{-1} at 103 K; 654 reflections with $F_o > 4\sigma(F)$ and $\sin\theta/\lambda < 0{\cdot}8$ Å^{-1} at 293 K]. Full-matrix least-squares refinements were carried out using Stewart's rigid pseudoatom model. Fixed neutron values were assumed for the nuclear positional parameters, and for selected thermal parameters (U_{ij} for H atoms and third-order c_{jkl} values for all atoms). The model gave a satisfactory fit to the X-ray data in terms of 150 variables which included population parameters for multipole expansions of the charge density as far as octapole terms for C and N atoms and quadrupoles for H atoms. Although ring-atom mean-square thermal vibrational amplitudes are considerably different at the two temperatures ($U \sim 0{\cdot}06$ Å^2 at 293 K; $U \sim 0{\cdot}02$ Å^2 at 103 K), the derived static charge distributions are in good agreement. This is attributed to the importance of the octapole deformation density for the imidazole-ring atoms. The charge density is consistent with a simple electrostatic theory for the strong NH···N hydrogen bond. It is also found that the approximate *2mm* symmetry in the molecular geometry extends to the charge distribution, and that there are similarities with the charge distribution in the imidazole ring of 9-methyladenine. [Crystal data: space group $P2_1/c$, $Z = 4$, $a = 7{\cdot}731$ (4), $b = 5{\cdot}453$ (2), $c = 9{\cdot}782$ (5) Å, $\beta = 117{\cdot}28$ (3)° at 293 K and $a = 7{\cdot}567$ (1), $b = 5{\cdot}371$ (1), $c = 9{\cdot}781$ (2) Å, $\beta = 119{\cdot}05$ (1)° at 103 K.]

Introduction

Imidazole has biological importance as a constituent of histamine, the histidine residues of proteins and the purine bases of nucleotides. The function of the imidazole ring hinges on the ease of its ionization ($pK_a = 6{\cdot}95$) in biological systems, and the possibilities for coupled gain and loss of protons at the two N atoms.

In connection with the present study of the electronic charge density in imidazole, the neutron crystal structure has been determined both at 293 K (Craven, McMullan, Bell & Freeman, 1977; hereafter CMBF) and at 103 K (McMullan, Epstein, Ruble & Craven, 1979; hereafter MERC). Earlier structure determinations were carried out from photographic X-ray data collected at 123 K (Martínez-Carrera, 1966) and room temperature (Will, 1969).

Experimental

(*a*) *The X-ray data collection*

Monoclinic crystals of imidazole have space group $P2_1/c$ with four molecules in the unit cell. Crystals exhibiting forms {100}, {110} and {001} were grown from benzene solution as described by CMBF. Those used for X-ray data collection at 293 and 103 K measured 0·2 × 0·2 × 0·5 and 0·38 × 0·44 × 0·44 mm respectively. The X-ray data were obtained using an Enraf–Nonius CAD-4 computer-controlled diffractometer with graphite-monochromated Mo $K\alpha$ radiation ($\lambda = 0{\cdot}7107$ Å). Crystals were mounted with the c^* axis within a few degrees of the diffractometer φ axis. Crystal cooling was by a stream of nitrogen gas from an Enraf–Nonius low-temperature device. The temperature was monitored (±2 K throughout data collection) using a thermocouple in the cold stream 8 mm from the crystal. In order to minimize ice formation on the crystal, the diffractometer was in a sealed plastic tent together with four containers of phosphorus pentoxide. A slight positive pressure of nitrogen gas was maintained. The crystal was also coated in clear varnish‡ to prevent dissolution in

* Present address: Research School of Chemistry, Australian National University, Canberra, ACT 2600, Australia.

† Author to whom correspondence should be addressed.

‡ Krylon Crystal Clear Spray Coating No. 1302; Krylon Inc., Norristown, PA.

0567-7408/82/010140-10$01.00

condensed moisture during periods of warming to room temperature. As described by MERC, the temperature for X-ray data collection (103 K) was estimated within about 5 K by a comparison of imidazole lattice parameters with those measured by neutrons at temperatures in the range 103 to 123 K. The lattice parameters used in the charge density refinements were $a = 7{\cdot}731\ (4)$, $b = 5{\cdot}453\ (2)$, $c = 9{\cdot}782\ (5)$ Å, $\beta = 117{\cdot}28\ (3)°$ at 293 K and $a = 7{\cdot}567\ (1)$, $b = 5{\cdot}371\ (1)$, $c = 9{\cdot}781\ (2)$ Å, $\beta = 119{\cdot}05\ (1)°$ at 103 K. These values were obtained by least-squares fitting of $\sin^2\theta$ values for 22 (293 K) and 40 (103 K) X-ray reflections in the range $12° < \theta < 32°$, each measured at $\pm\theta$. Similar measurements with a standard sodium chloride crystal at 293 K, assuming $a_0 = 5{\cdot}6402$ Å, gave a calculated wavelength 0·7093 (1) Å corresponding to Mo $K\alpha_1$. Hence this wavelength was used in obtaining the imidazole lattice parameters.

Integrated intensities were measured by $\theta/2\theta$ scans with scan widths $\Delta\theta(°) = 1{\cdot}2 + 0{\cdot}9\tan\theta$ at 293 K and $2{\cdot}0 + 0{\cdot}9\tan\theta$ at 103 K. Three monitoring reflections were remeasured after every fifty (293 K) or twenty (103 K) reflections. The overall variation in intensity for these reflections was 2%. No X-ray absorption corrections were applied.

At 293 K, intensities were measured for 2218 non-symmetry-related reflections with $\sin\theta/\lambda < 0{\cdot}83$ Å^{-1}. At 103 K, intensities were measured for 3279 non-symmetry-related reflections with $\sin\theta/\lambda < 1{\cdot}30$ Å^{-1}. For reflections with $\sin\theta/\lambda > 1{\cdot}0$ Å^{-1} only those were measured which gave a quasi-normalized structure amplitude $|E(hkl)| \geq 2$ in a calculation based on the neutron structure previously determined by CMBF.

(*b*) *The X-ray structure refinements*

The electronic charge density refinements at each temperature were based on the rigid pseudoatom model of Stewart (1976). Initially, this involved the usual atomic positional and anisotropic thermal parameters, U_{ij}. Fixed neutron values (CMBF and MERC) were assumed for all positional parameters and for H-atom anisotropic thermal parameters. Atomic nomenclature (Fig. 1 and Table 1) is consistent with CMBF and MERC. Pseudoatom X-ray scattering factors are described in the Appendix.* Except in the final refinements described in section (*e*), the pseudoatoms were assumed to consist of spherical *K*-shell cores (Clementi, 1965) with valence-shell charge density having a radial distribution of the Slater type. Thus, each of the three atom types (C, N and H) required one variable radial exponent (α). Each pseudoatom also involved 16 population parameters (9 for H atoms) to specify populations for the various angular terms in the valence charge density. No X-ray extinction correction was used. The full-matrix least-squares refinement was carried out with the computer program of Craven & Weber (1977), so as to minimize the function $\sum w\Delta^2$ where $\Delta = |F_o| - |F_c|$ and $w = \sigma^{-2}(F_o)$. At first, the variances were assumed from $\sigma^2(I) = \sigma^2 + (0{\cdot}02I)^2$ where I is the observed integrated intensity and σ^2 is the variance due to counting statistics. Initial refinement using 103 K data gave convergence with $R_w = 0{\cdot}029$, $R = 0{\cdot}032$ and QME = 1·254.* It was noted that values of $|\Delta|/\sigma(F)$ became systematically large for reflections with small $|F_o|$ values. This seemed to be caused in two ways. First, the values used for $\sigma(F)$ appeared to be underestimated for the smaller values of $|F_o|$. Proceeding as in the study of 9-methyladenine

* Refinement criteria are $R = \sum_H|\Delta|/\sum_H|F_o|$; $R_w = (\sum_H w\Delta^2/\sum_H w|F_o|^2)^{1/2}$; and QME $= [\sum_H w\Delta^2/(n_o - n_{\text{param}})]^{1/2}$.

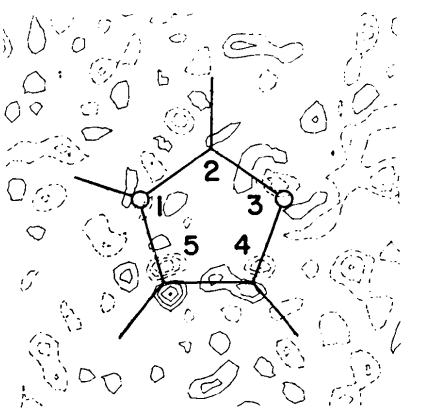

(*a*)

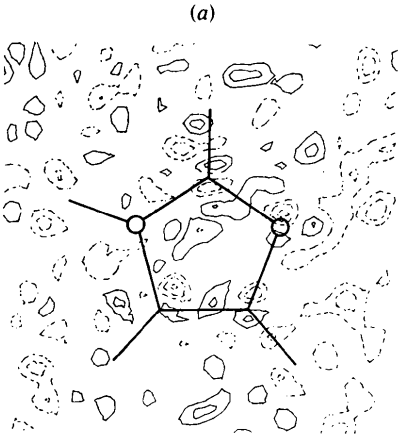

(*b*)

Fig. 1. Sections of difference Fourier syntheses in the ring plane showing the residual charge densities for refinements using the data collected at 103 K. Contours are at intervals of 0·05 e Å^{-3} with the zero contour omitted and negative contours shown dotted. The average e.s.d. in residual density is 0·04 e Å^{-3}. Values at points of interest are given in the text. The molecular framework is shown with the ring-numbering system. The N atoms are open circles. (*a*) Refinement 103 S, which does not include thermal parameter values c_{jkl}. (*b*) Refinement 103 SC which includes c_{jkl} values, as determined from the neutron data.

* Further details of preliminary structure refinements and results have been given by Epstein (1978).

(Craven & Benci, 1981), variances for all 103 K data were revised based on a least-squares fit of duplicate intensity measurements for 115 reflections. This gave $\sigma^2(F) = (383 - 20{\cdot}1|F_o| + 1{\cdot}28|F_o|^2) \times 10^{-4}$. Second, the values of $|\Delta|$ showed a systematic trend for the very weak reflections. Of all 2206 reflections with $F > 3\sigma$ at 103 K, there were a total of 41 with $|\Delta|/\sigma$ ranging from 3·0 to a maximum of 7·5. It was noted among these that $|F_o| > |F_c|$ for every one of the 22 reflections $|F_o| < 3{\cdot}0$.* No satisfactory explanation of this could be found in terms of the assumed model. It was concluded that $|F_o|$ values for the very weak reflections tended to be overestimated. Re-examination of the intensity scans showed nothing unusual. Although the effect might be due to multiple Bragg

* Lists of structure factors, including a separate table of the reflections with $|\Delta|/\sigma > 3$, and atomic parameters for the refinements 103 SC, 293 SC which are described in section (*d*), have been deposited with the British Library Lending Division as Supplementary Publication No. SUP 36243 (34 pp.). Copies may be obtained through The Executive Secretary, International Union of Crystallography, 5 Abbey Square, Chester CH1 2HU, England.

Table 1. *Atomic positional and thermal parameters*

(*a*) Nuclear positional parameters

These values ($\times 10^4$) are from new refinements using neutron data at 103 K (top) and 293 K (bottom). The data were those of McMullan, Epstein, Ruble & Craven (1979) and Craven, McMullan, Bell & Freeman (1977). There are some possibly significant differences from their positional parameters ($<2{\cdot}5\sigma$), associated with the inclusion of c_{jkl} thermal parameters, (*c*) below.

	x	*y*	*z*		*x*	*y*	*z*
N(1)	2189 (1)	3327 (2)	872 (1)	C(4)	3091 (2)	5524 (3)	2990 (2)
	2193 (3)	3302 (5)	881 (3)		3076 (5)	5436 (7)	2969 (4)
H(1)	2030 (4)	2673 (6)	−186 (4)	H(4)	3696 (5)	6897 (7)	3894 (4)
	2043 (7)	2674 (12)	−152 (7)		3682 (12)	6785 (15)	3863 (8)
C(2)	1567 (2)	2183 (3)	1790 (2)	C(5)	3166 (2)	5456 (3)	1619 (2)
	1581 (4)	2223 (7)	1809 (4)		3144 (5)	5372 (8)	1603 (4)
H(2)	781 (5)	455 (7)	1497 (4)	H(5)	3824 (5)	6718 (6)	1135 (4)
	827 (11)	557 (14)	1559 (8)		3786 (11)	6594 (14)	1113 (9)
N(3)	2085 (1)	3459 (2)	3090 (1)				
	2089 (3)	3452 (4)	3094 (2)				

(*b*) Anisotropic thermal parameters, U_{ij} (units $Å^2 \times 10^4$)

The temperature-factor expression is $T = \exp(-2\pi^2 \sum_i \sum_j \mathbf{h}_i \mathbf{h}_j a_i^* a_j^* U_{ij})$. For each atom, the rows are for refinements: (1) neutron data, 103 K, (2) X-ray data, 103 K, (3) neutron data, 293 K, (4) X-ray data, 293 K. For H atoms, the rows are for the neutron values only.

	U_{11}	U_{22}	U_{33}	U_{12}	U_{13}	U_{23}
N(1)	200 (2)	198 (2)	114 (2)	1 (1)	101 (1)	−7 (1)
	174 (2)	178 (2)	110 (2)	−5 (2)	89 (2)	−11 (2)
	572 (4)	612 (6)	365 (5)	10 (4)	278 (4)	−13 (4)
	557 (18)	603 (19)	279 (14)	−3 (15)	255 (2)	−14 (14)
H(1)	390 (6)	356 (6)	200 (6)	−33 (5)	184 (4)	−48 (5)
	841 (16)	887 (18)	456 (15)	−58 (13)	375 (13)	−61 (15)
C(2)	224 (2)	182 (3)	144 (2)	−24 (2)	117 (2)	−8 (2)
	197 (3)	168 (3)	139 (2)	−26 (2)	104 (2)	−11 (2)
	648 (8)	573 (9)	442 (6)	−61 (6)	327 (6)	−30 (6)
	631 (17)	558 (18)	401 (15)	−60 (11)	333 (13)	4 (13)
H(2)	598 (8)	338 (7)	403 (7)	−188 (6)	278 (6)	−82 (5)
	1286 (29)	895 (27)	908 (21)	−437 (23)	614 (20)	−177 (20)
N(3)	262 (2)	218 (2)	135 (2)	−9 (1)	139 (1)	2 (1)
	236 (3)	199 (3)	136 (2)	−11 (3)	131 (2)	−2 (2)
	756 (6)	667 (6)	400 (5)	−9 (5)	378 (4)	10 (4)
	711 (19)	654 (20)	352 (16)	−1 (18)	367 (14)	45 (16)
C(4)	284 (3)	197 (2)	142 (3)	−32 (2)	129 (2)	−35 (2)
	258 (3)	181 (3)	140 (2)	−32 (2)	117 (2)	−35 (2)
	822 (9)	607 (8)	452 (7)	−75 (7)	351 (6)	−89 (6)
	808 (22)	573 (17)	417 (17)	−47 (15)	366 (15)	−62 (15)
H(4)	709 (10)	405 (8)	343 (7)	−176 (7)	297 (7)	184 (6)
	1622 (34)	1044 (26)	826 (21)	−394 (23)	667 (22)	−427 (21)
C(5)	257 (2)	198 (2)	149 (3)	−33 (2)	132 (2)	−2 (2)
	229 (3)	180 (3)	157 (2)	−34 (2)	126 (2)	−1 (2)
	748 (8)	602 (9)	499 (7)	−77 (7)	374 (6)	19 (7)
	732 (20)	559 (17)	451 (16)	−105 (14)	374 (14)	8 (16)
H(5)	619 (9)	435 (7)	425 (8)	−186 (6)	355 (7)	9 (6)
	1558 (33)	1052 (26)	987 (22)	−422 (23)	850 (24)	−20 (18)

Table 1 (*cont.*)

(*c*) Third-order atomic thermal parameters, c_{jkl} ($\times 10^7$)

The temperature-factor expression is $T = -\frac{4}{3}\pi^3 i \sum_j \sum_k \sum_l \mathbf{h}_j \mathbf{h}_k \mathbf{h}_l c_{jkl}$. For each parameter, the top value is from neutron data at 103 K (MERC) and the bottom value from neutron data at 293 K (CMBF). Values marked with an asterisk are different from zero by at least 3σ.

	c_{111}	c_{222}	c_{333}	c_{112}	c_{122}	c_{113}	c_{133}	c_{223}	c_{233}	c_{123}
N(1)	−5 (4)	3 (9)	2 (3)	0 (3)	0 (3)	−1 (2)	1 (2)	1 (3)	1 (2)	0 (2)
	10 (12)	−57 (37)	−6 (7)	11 (10)	−12 (14)	−1 (6)	−2 (6)	−2 (11)	7 (7)	2 (6)
H(1)	−3 (15)	2 (29)	−2 (10)	12 (11)	−2 (12)	9 (8)	3 (7)	10 (9)	0 (7)	3 (6)
	22 (43)	104 (114)	32 (21)	−6 (37)	−59 (44)	12 (20)	17 (17)	9 (37)	31 (22)	−8 (20)
C(2)	−2 (6)	−25 (13)	0 (4)	−6 (4)	−18 (6)*	−1 (3)	−1 (3)	−11 (4)	0 (3)	−1 (2)
	−23 (20)	119 (52)	−14 (10)	44 (17)	−53 (20)	−16 (10)	−13 (8)	−32 (18)	13 (10)	30 (10)*
H(2)	53 (23)	51 (36)	−22 (11)	23 (15)	7 (18)	1 (12)	−3 (9)	−3 (12)	13 (8)	14 (9)
	314 (93)*	610 (177)*	44 (29)	93 (71)	−82 (74)	75 (43)	32 (30)	−15 (53)	34 (31)	45 (37)
N(3)	−1 (4)	0 (8)	−1 (3)	−1 (3)	7 (3)	−1 (3)	0 (2)	6 (3)	4 (2)	2 (2)
	−36 (15)	−43 (39)	1 (7)	−33 (12)	7 (15)	−18 (7)	−9 (5)	4 (10)	3 (6)	2 (7)
C(4)	−12 (7)	2 (13)	1 (4)	3 (5)	−1 (5)	−1 (4)	1 (3)	1 (4)	3 (3)	2 (3)
	−65 (25)	−112 (55)	−1 (12)	−22 (19)	−12 (23)	−9 (12)	3 (9)	11 (15)	−4 (9)	6 (10)
H(4)	−91 (28)*	−135 (38)*	−13 (11)	−4 (18)	18 (20)	−32 (14)	−15 (10)	23 (15)	2 (10)	12 (10)
	−406 (114)*	−376 (174)	−30 (30)	43 (81)	138 (91)	−134 (51)	−58 (33)	89 (63)	20 (33)	20 (42)
C(5)	−11 (6)	−15 (12)	−3 (4)	−4 (4)	−11 (5)	−6 (4)	−4 (3)	−6 (4)	−4 (3)	2 (3)
	−84 (23)*	10 (56)	−13 (11)	−6 (18)	−3 (23)	−46 (11)*	−25 (8)*	−21 (16)	−25 (10)	−15 (10)
H(5)	−116 (25)*	−73 (37)	−29 (11)	−2 (17)	1 (19)	−61 (14)*	−36 (10)*	−27 (13)	−5 (9)	−8 (10)
	−523 (111)*	−203 (166)	−30 (32)	169 (82)	−115 (84)	−276 (55)*	−127 (37)*	−30 (53)	−25 (33)	−8 (41)

reflection or to thermal diffuse scattering, this was not proven. A similar but less striking effect was observed for the 293 K data. In subsequent refinements, many of these weak reflections were omitted by raising the acceptance threshold for all reflections so that $F > 6\sigma$ for 103 K data and $F > 4\sigma$ for 293 K data. Refinements for the determination of 150 structure variables were continued, based on 1892 reflections measured at 103 K and 654 at 293 K. Among these were 668 reflections at 103 K with $\sin\theta/\lambda \geq 0{\cdot}65$ Å^{-1} and 104 at 293 K. Convergence was obtained with $R_w = 0{\cdot}028$, $R = 0{\cdot}031$ and QME = 1·189 for 103 K data and $R_w = 0{\cdot}015$, $R = 0{\cdot}026$ and QME = 1·091 for 293 K data. Henceforth, these refinements are called 103 S and 293 S respectively. Final difference Fourier syntheses showed no significant residual density in the 293 K map. However, in the 103 K map (Fig. 1*a*), there are significant features ($+3\sigma$, -4σ) close to atom C(5). Since these features were absent in a map including only reflections with $\sin\theta/\lambda < 0{\cdot}65$ Å^{-1}, it was concluded that they may be due to small apparent differences in nuclear positions as determined by neutron and X-ray diffraction due to an inadequate model either for the atomic thermal motion or for the charge density close to the atom centers.

(*c*) *Neutron structure refinements with thermal parameters, c_{jkl}*

In the crystal structure of parabanic acid (Craven & McMullan, 1979), similar residual density features were observed at carbonyl O atoms. An effort was made to include them in the structure model by introducing third-order thermal parameters (c_{jkl}, as defined by equation 5.2.3.9; Johnson & Levy, 1974) with values determined from the neutron data. For parabanic acid, this was unsuccessful, presumably because the c_{jkl} values were not sufficiently accurate. In the case of imidazole, new refinements were carried out using the neutron data at 103 K (MERC) and 293 K (CMBF). Convergence was obtained with $R_w = 0{\cdot}020$, $R = 0{\cdot}026$ and QME = 1·324 for 103 K and $R_w = 0{\cdot}026$, $R = 0{\cdot}025$ and QME = 1·004 for 293 K. The final neutron parameter values are in Table 1. The *R*-factor-ratio test (Hamilton, 1974) indicated that the additional ten c_{jkl} parameters per nucleus gave an improvement which was significant at higher than the 99·5% level of confidence. The revised structure model produced the greatest effect at the H nuclei, which was to be expected, since these have greater amplitudes of thermal motion than the nuclei in the imidazole ring. In addition to having several significantly non-zero c_{jkl} values, there were also changes in the apparent nuclear positions,* the greatest being 0·015 Å (4σ) for both H(2) and H(5) at 103 K and 0·03 Å (4σ) for H(2) at 293 K. The shift at C(5) of 0·004 Å (2σ) at 103 K was the most significant among those of the ring nuclei. The changes in U_{ij} values were negligible for all nuclei at both temperatures.

(*d*) *X-ray structure refinements with revised model for thermal motion*

Refinements were then carried out using the X-ray data with the same variables as in refinements 103 S and 293 S. However, the nuclear positional parameters and the complete set of values for the c_{jkl} thermal parameters were also included with fixed values from

* There was about a threefold increase in e.s.d.'s for positional parameters compared with those given by MERC and CMBF. This is associated with the strong correlations (c_{111} with x, c_{222} with y and c_{333} with z) which range in value from 0·67 to 0·86.

the new neutron refinements. Convergence for these refinements (henceforth 103 SC and 293 SC) was obtained with $R_w = 0{\cdot}028$, $R = 0{\cdot}031$, QME = 1·203 for the 103 K data and $R_w = 0{\cdot}015$, $R = 0{\cdot}027$, QME = 1·104 for the 293 K data. Thus the revised model for describing the thermal motion had little effect on the overall agreement between observed and calculated X-ray structure amplitudes. In the difference Fourier synthesis (Fig. 1*b*) the residual maximum density near atom C(5) has gone. The adjacent negative density feature remains as the most significant (4σ) in the map. The trough is smaller than in Fig. 1(*a*), but it is centered further from the C(5) nuclear position, so that the e.s.d. in the residual density is smaller (0·04 *vs* 0·06 e Å^{-3}).

It is notable that although these refinements produced differences as much as 0·2 e Å^{-3} at corresponding points in the two residual density maps (Fig. 1*a*, *b*), these are associated with small differences in F_{calc} involving reflections with $\sin\theta/\lambda > 0{\cdot}65$ Å^{-1}. The revised model for thermal motion gave no significant changes either in the electronic population parameters which describe the valence charge density or in the anisotropic temperature factors U_{ij}.* However, as found in other similar structure refinements (Craven & McMullan, 1979; Craven & Benci, 1981), the X-ray and neutron values for U_{ij} are systematically different. In this case, the X-ray values for U_{ii} are smaller for the refinements at both temperatures. The reason for these effects remains obscure.

(*e*) *X-ray refinements using pseudoatoms with Hartree–Fock cores*

The refinements 103 SC and 293 SC previously described, in which the complete valence-shell charge density was based on Slater-type radial functions, were found to give a net molecular valence charge (Σp_v) of 23·8 (2) e (103 K) or 25·5 (3) e (293 K) when p_v values were varied without constraint. This indicated a deficiency of charge for the 103 SC refinement compared with the expected value (26 valence electrons) for a neutral molecule. Since the charge obtained for a pseudoatom depends on the nature of the assumed

* See deposition footnote.

Table 2. *Electron population parameters* ($\times 10^2$)

These are coefficients for the expression which is given in the Appendix. They are given with respect to a molecular Cartesian axial system with x along the C(5) → C(4) bond and z normal to the ring plane (*i.e.* up from the page in Fig. 3). These values (103 K on top, 293 K below) are from the refinements 103 H and 293 H, based on isolated Hartree–Fock atomic scattering factors for f_{core}. The fixed values of the radial exponents (α) were 3·90, 3·26 and 2·40 bohr^{-1} for N, C and H pseudoatoms respectively.

	p_v	d_1	d_2	d_3	q_1	q_2	q_3	q_4	q_5
N(1)	5 (4)	1 (1)	1 (1)	−2 (1)	−10 (1)	0 (1)	−6 (1)	−2 (2)	2 (1)
	7 (12)	−4 (2)	−5 (2)	0 (2)	5 (6)	−7 (7)	7 (5)	−9 (7)	−4 (5)
H(1)	−29 (2)	21 (1)	−8 (2)	3 (2)	8 (1)	8 (2)	6 (2)	−1 (2)	−11 (2)
	−19 (4)	15 (2)	−1 (3)	−5 (3)	14 (2)	2 (2)	−2 (3)	3 (3)	−10 (3)
C(2)	2 (5)	3 (1)	1 (2)	0 (1)	−11 (2)	−4 (2)	−5 (1)	−2 (2)	−10 (1)
	39 (13)	12 (3)	−9 (3)	3 (3)	6 (5)	7 (5)	0 (5)	−4 (6)	−19 (5)
H(2)	−3 (3)	0 (2)	−14 (2)	4 (2)	−6 (2)	3 (2)	−4 (2)	6 (2)	−3 (2)
	−3 (5)	−8 (3)	−19 (3)	0 (3)	−4 (3)	8 (3)	3 (3)	−2 (3)	−7 (2)
N(3)	12 (3)	7 (1)	3 (1)	2 (1)	−4 (2)	4 (2)	−9 (1)	0 (2)	−3 (1)
	9 (10)	6 (2)	−2 (3)	2 (2)	9 (6)	13 (7)	2 (5)	−7 (8)	0 (6)
C(4)	2 (5)	2 (1)	−2 (2)	0 (2)	−7 (2)	−4 (2)	−5 (2)	0 (2)	−9 (2)
	25 (14)	−5 (3)	1 (3)	−1 (3)	8 (5)	12 (6)	6 (6)	1 (7)	−8 (6)
H(4)	−8 (3)	−10 (2)	9 (2)	−3 (2)	−6 (2)	−9 (2)	3 (2)	−3 (2)	3 (2)
	3 (6)	−8 (3)	19 (4)	−1 (3)	−5 (3)	−6 (3)	−4 (3)	−1 (3)	−8 (3)
C(5)	24 (5)	8 (1)	−11 (1)	2 (1)	−5 (2)	13 (2)	−10 (2)	0 (2)	−6 (2)
	24 (14)	1 (3)	−6 (3)	2 (3)	−3 (5)	2 (5)	3 (6)	−1 (7)	−18 (6)
H(5)	−15 (3)	5 (2)	4 (2)	0 (2)	−3 (2)	1 (2)	−3 (2)	1 (2)	1 (2)
	−15 (5)	6 (3)	12 (3)	0 (3)	−2 (3)	0 (3)	5 (3)	−3 (3)	2 (3)

	o_1	o_2	o_3	o_4	o_5	o_6	o_7
N(1)	−7 (1)	19 (1)	−2 (1)	−1 (1)	1 (1)	3 (2)	1 (1)
	−13 (7)	18 (7)	8 (8)	−3 (7)	2 (8)	2 (9)	−1 (7)
C(2)	−5 (2)	−28 (2)	4 (2)	−2 (2)	3 (2)	4 (2)	0 (2)
	−3 (7)	−41 (8)	0 (10)	3 (9)	−1 (11)	7 (10)	1 (11)
N(3)	8 (1)	8 (1)	0 (1)	3 (2)	1 (1)	−1 (1)	0 (1)
	6 (7)	−3 (8)	−2 (7)	−5 (9)	4 (7)	−1 (8)	−2 (10)
C(4)	−20 (2)	−7 (2)	2 (2)	0 (2)	−4 (2)	0 (2)	0 (2)
	−34 (8)	3 (8)	2 (9)	−2 (12)	−5 (9)	−1 (11)	−1 (12)
C(5)	29 (2)	−16 (2)	−2 (2)	−2 (2)	0 (2)	3 (2)	0 (2)
	25 (8)	−11 (8)	0 (10)	−2 (10)	0 (9)	−2 (12)	−3 (11)

radial density function, it was of interest to consider a different structure model. The alternative model was chosen to be closely related to that of a conventional structure refinement. The pseudoatoms were represented by Hartree–Fock isolated atoms (Cromer & Waber, 1965) with only the asphericity and the departure from atomic neutrality represented by terms involving Slater-type charge density radial functions. For hydrogen, spherical bonded-atom X-ray scattering factors were assumed (Stewart, Davidson & Simpson, 1965). In this model, the radial exponents, α, were assigned fixed values 3·90, 3·26, 2·4 bohr^{-1} (the Bohr radius is 52·92 pm) for N, C and H atoms respectively, these being the values obtained in the previous 103 K refinements. Otherwise, the structure model was unchanged. Refinements (henceforth 103 H and 293 H) converged with $R_w = 0{\cdot}028$, $R = 0{\cdot}031$, QME = 1·208 for 103 K data and $R_w = 0{\cdot}015$, $R = 0{\cdot}026$, QME = 1·113 for 293 K data. In these refinements, positive and negative values of p_v represent an excess or deficiency of electronic charge with respect to a neutral atom. Values of the net molecular charge Σp_v were −0·1 (1) e (103 K) and +0·7 (3) e (293 K). According to this structure model, the net molecular charge is insignificantly different from zero in both refinements. A comparison with refinements 103 SC and 293 SC showed that the results were very similar. There were systematic increases (1 to 7%) in the values of anisotropic temperature factors U_{ii}, but no significant differences in the Fourier syntheses of residual density. When the values of the population parameters from 103 SC and 293 SC were normalized to be consistent with a neutral molecule, there were no significant differences in the d_i, q_i and o_i values from those obtained with the Hartree–Fock model. Also, it should be noted that the refinement criteria were essentially unchanged.

Because of the convenience in making comparisons of the results obtained for 103 and 293 K, we report values of the structure parameters obtained based on the Hartree–Fock model (Tables 1, 2).

Comparison of results at 103 and 293 K

In applying the pseudoatom model, it is assumed that the electronic charge associated with each nucleus follows the nucleus rigidly throughout its thermal motion (Stewart, 1976). If this is true, and if the thermal motion is properly described, then a static charge density distribution for imidazole can be mapped which should be the same within experimental error for the structure at 293 and 103 K. Calculations for diatomic molecules show that non-rigidity should have small effect on the charge density parameters determined from X-ray diffraction data (Epstein & Stewart, 1979*a*, *b*). In the case of imidazole, this may not be true because the molecule is more complex, with larger thermal vibrational amplitudes, even at 103 K. It is also possible that the static charge density maps are affected by systematic errors in the X-ray and neutron diffraction data. Thus, the comparison of maps for imidazole obtained at 293 and 103 K is considered to provide a severe test of the quality of the data and of the pseudoatom model.

The maps of total static valence charge obtained at the two temperatures are very similar. Only the map for 103 K is shown (Fig. 2). The two maps of deformation density are also similar (Fig. 3*a*, *b*), although there are differences (Fig. 3*c*) which are possibly significant in terms of their e.s.d.'s. Such differences can also be seen in the values of the electron population parameters (Table 2). Much of the error in these differences comes from the refinement at 293 K. This is attributed to the large amplitude of atomic thermal vibrations at 293 K (Table 1, see also Fig. 1 in MERC) which limited the number of reflections with $\sin\theta/\lambda > 0{\cdot}6$ Å^{-1} that could be measured. Since the valence charge density contributions only become small at $\sin\theta/\lambda > 0{\cdot}6$ Å^{-1}, there is a resulting difficulty in deconvoluting the charge density from the thermal motion. Under circumstances in which a charge density analysis would not usually be undertaken, the agreement between the 293 K map and the more precise 103 K map is considered to be surprisingly good. It was noted that most of the differences between the maps could be attributed to the disagreement in values for a few dipole and quadrupole population parameters, which are marked in the deposited table of atomic parameters. These populations are strongly correlated with the values of the positional and anisotropic thermal

Fig. 2. Total valence charge for the static molecule, as determined at 103 K from refinement 103 S. Contours are at intervals of 0·2 e Å^{-3}. The ring atoms lie in troughs and the H atoms are at peaks. This is because the radial density functions for C and N atoms are zero at the atom centers. For details, see the Appendix. The e.s.d. is a maximum at about 0·3 Å from C and N atoms having the largest value 0·3 e Å^{-3} near N(3). Values at H atoms and at bond midpoints are about 0·1 e Å^{-3}.

parameters respectively.* Much of the agreement between the maps (Fig. 3*a*, *b*) is attributed to the good agreement obtained for the octapole populations, which are free from such strong correlations. There are no significant differences between the octapole charge density map for 103 K (Fig. 3*d*) and that for 293 K (not shown). The octapole deformations of the charge density, which in general are important for describing trigonal or tetrahedral bonding, are indeed robust components of the total electronic charge density. These features were important for prompting the early developments of charge density studies. They were noticed, although not so described, in difference Fourier maps following conventional spherical-atom refinements based on limited X-ray diffraction data. In a recent study of dimethylglyoxime (Craven, Chang & Ghosh, 1979), using only Cu $K\alpha$ X-ray intensity data ($\sin\theta/\lambda < 0{\cdot}65$ Å^{-1}), a refinement including octapole terms was used to distinguish the tetrahedral distribution of the valence charge at the oxime O atom from the trigonal distribution at the N.

Some caution is needed before concluding that deconvolution of thermal motion from the static charge density for other molecules will be as successful as in the case of imidazole. Further examples need to be studied, particularly molecules containing carbonyl groups, which characteristically have important quadrupole deformation density (Craven & McMullan, 1979).

* Correlation factors between U_{ij} and q_k parameters range up to 0·9 for the 293 K refinements, but are less (0·7) for the 103 K refinement since there are more reflections at $\sin\theta/\lambda > 0{\cdot}65$ Å^{-1}.

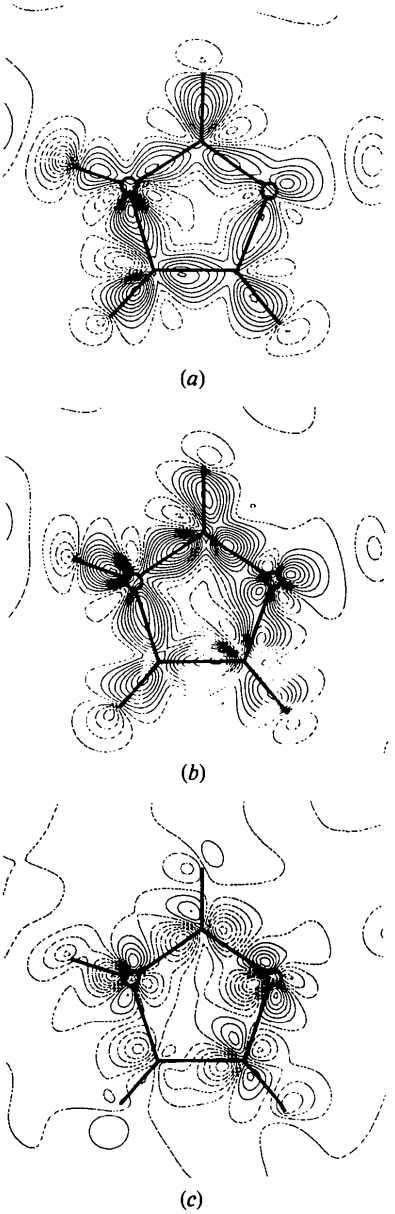

(*a*)

(*b*)

(*c*)

Fig. 3. Maps of charge density for the molecule at rest. The 'promolecule' consisting of Hartree–Fock isolated atoms has been subtracted. Contours are at intervals 0·1 e Å^{-3} with negative dotted contours corresponding to regions of electron deficiency. (*a*) Refinement at 103 K. Values of the e.s.d. are about 0·07 e Å^{-3} at the peaks (troughs). (*b*) Refinement at 293 K. The e.s.d.'s are 0·15 e Å^{-3} at the peaks (troughs). (*c*) The difference obtained by subtracting map (*b*) from (*a*). The residual charge becomes significant beyond the fourth contour level.

Hydrogen bonding and the valence charge density in imidazole

Having established that the room- and low-temperature results are consistent, we now confine our attention to the more precise low-temperature results. Net atomic charges (p_v, Table 2) are not significantly different from those of neutral atoms, except for the H atom H(1). Since the absolute values of these charges are model-dependent (Bentley & Stewart, 1975), the physical significance of such charges should be restricted to

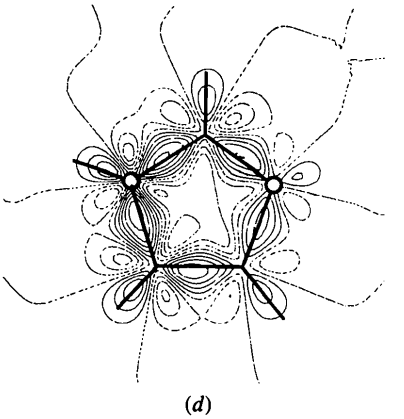

(*d*)

Fig. 3. (*cont.*) (*d*) Deformation map including only the octapole terms. This was obtained for the refinement at 103 K, the map for 293 K being very similar.

a comparison of relative values for pseudoatoms of the same kind. Thus, there is a depletion of charge (*i.e.* more negative p_v value) at the N—H hydrogen atom, $p_v = -0{\cdot}29\ (2)$ e, compared with the H atoms in C—H groups, $p_v = 0{\cdot}02\ (5)$, $-0{\cdot}08\ (3)$, $-0{\cdot}15\ (3)$ e. This is the most notable difference between the H atom which is hydrogen bonded, and the others which are not. The charges on the hydrogen-bond donor and acceptor N atoms are the same within experimental error, so that any sharing of charge from the hydrogen would be about equal. Both N atoms may have a small negative charge, consistent with an electrostatic model for the hydrogen bond. However, the magnitude of this charge is barely significant and is also subject to the nature of the charge density radial functions which have been assumed.

It is of interest to compare the dipole charge deformations for H atoms bonded to N and C. In all cases these deformations have maximum effect close to the N—H and C—H bond axis and act to enhance the electronic charge within the covalent-bond region. The magnitude of charge transfer after renormalization (see Table 3) is estimated as $(\Sigma_j^3 d_j^2)^{1/2}$. Values are 0·24, 0·15, 0·15, 0·07 for H(1), H(2), H(4) and H(5) respectively, with e.s.d.'s of 0·02. Thus the dipole deformation at the hydrogen-bonded H(1) may be significantly greater than that at H atoms of C—H groups. However, in 9-methyladenine (Craven & Benci, 1981), the effect is in the opposite sense, with N—H hydrogen atoms having smaller dipole deformations (0·08, 0·09) than the ring C—H hydrogen atoms (0·19, 0·20; $\sigma = 0{\cdot}03$). This effect may be due to the shorter hydrogen bond in imidazole (H···N distance 1·81 Å, $\sigma < 0{\cdot}01$ Å; MERC) compared with those in 9-methyladenine (H···N distances 1·95 Å, $\sigma < 0{\cdot}01$ Å; McMullan, Benci & Craven, 1980).

Table 3. *Electron population parameters for 9-methyladenine in the molecular fragment in common with imidazole*

Atomic nomenclature is that of imidazole, rather than 9-methyladenine. Values of population parameters ($\times 10^2$) for 9-methyladenine at 126 K (Craven & Benci, 1981) have been transformed by rotation from the crystal axial system *a*, *b*, *c** using the procedure of Cromer, Larson & Stewart (1976), so that they are referred to a right-handed molecular Cartesian axial system with *x* along the C(5) → C(4) bond and *z* normal to the ring. The values have also been renormalized (Hansen & Coppens, 1978) as described in the Appendix. The e.s.d.'s for all values range from 0·02 to 0·03.

	d_1	d_2	d_3	q_1	q_2	q_3	q_4	q_5
C(2)	5	−10	−6	−2	−5	5	−1	−7
H(2)	−2	−19	−3	−2	−2	−7	−5	−13
N(1)	3	−4	−4	1	−5	5	−1	2
N(3)	8	2	−4	8	−1	1	3	−7
C(5)	6	−4	−3	5	6	3	1	−10
C(4)	−7	−6	12	5	−3	2	0	−7

	o_1	o_2	o_3	o_4	o_5	o_6	o_7
C(2)	0	−24	1	0	7	5	4
N(1)	−11	14	0	2	8	2	1
N(3)	6	8	2	−1	8	4	5
C(5)	20	−7	−2	−4	2	6	1
C(4)	−24	−4	−4	−1	4	7	−2

Although the dipole deformations are predominant for the H atoms, certain octapole and quadrupole deformations are more important for the ring atoms. In particular, the largest parameter values are for the octapole terms o_1 and o_2 which both have trigonal symmetry. The threefold axis for each of these deformation terms passes through the atom center and is perpendicular to the imidazole ring. These terms combine to form maximum bonding density in the σ region between atoms. Terms involving o_5 and o_6 contribute to π-bonding density, but these values are considerably smaller. As expected, values for o_3, o_4 and o_7 are negligibly small because these are for deformations which are antisymmetric with respect to the ring plane. Other deformations which are antisymmetric in this way are the quadrupole terms involving q_3 and q_4. There are significantly non-zero values of q_3 for atoms N(3) and C(5) which enhance the deformation density above the plane of the molecule in the region of the re-entrance N(1)—C(5)—H(5) and distort the non-bonding density region at N(3) away from the line of N(3)···H(1)N(1) hydrogen bonding. The maximum discrepancy is 0·28 (7) e Å^{-3} at corresponding points ±0·4 Å from the ring plane. Although the packing arrangement is markedly different above and below the molecular plane (Fig. 3 in CMBF), there is no apparent explanation for these small but significant effects on the charge density. Terms involving q_1 and q_2 have $2/m$ symmetry with twofold axes through the atom centers and perpendicular to the ring. Thus they affect the σ-bonding density. Negative values for q_5 act to deplete charge from both sides of the ring plane at each atom center. Such effects are of marginal significance for the C atoms of imidazole, but are an important feature of the deformation density at carbonyl C atoms, as in parabanic acid (Craven & McMullan, 1979) and barbital (Fox, Weber & Craven, 1982).

In discussing the neutron determination of bond lengths and angles in imidazole, CMBF noted that except for the presence of the H(1) atom, the molecule conformed closely to the symmetry *2mm*. It was suggested that proton transfer from N(1) to N(3) or proton addition at N(3) would not involve a major change in the imidazole charge density distribution. Such reactions are biologically important because of the part played by the imidazole of a histidine residue in the charge-relay system of proteases (Blow, 1976). The approximate *2mm* symmetry of imidazole can be seen in the total valence charge distribution (Fig. 2). Small but significant differences between the left and

right sides of the molecule occur in the deformation map (Fig. 3). However, the extent of the pseudosymmetry is more clearly revealed in comparing population parameters (Table 2), because the contribution to the charge density from hydrogen atom H(1) can be conveniently neglected. In comparing atoms N(1) with N(3) and C(5) with C(4), a sign change is necessary for each of the terms d_1, q_2, q_3, o_1, o_4, o_5, which are antisymmetric with respect to the plane normal to the ring and passing through C(2) and H(2). These terms should be zero for C(2) and H(2). Much of the pseudosymmetry appears to come from the large values of either o_1 or o_2 which contribute to the charge density in the σ-bonding regions between ring atoms.

The electron population parameters (Table 3) also provide a convenient comparison of the charge density in imidazole with the imidazole portion of 9-methyladenine (Craven & Benci, 1981). Of course there are important chemical differences involved since the ring substituent atoms at positions N(1), C(4) and C(5) are H atoms in imidazole and C atoms in 9-methyladenine. However, at the atoms which are common, there are similarities in the charge deformations which are strongest for the octapole terms. It is premature to discuss such a comparison in detail. The present purpose is to point to the potential use of the pseudoatom model for deriving a quantitative experimental description of the charge in molecular fragments or functional chemical groupings. It remains to determine how well such descriptions can be transferred from one crystal structure to another, or eventually into a non-crystalline environment.

We thank Dr R. F. Stewart for his interest and particularly for his encouragement of one of us (JE) in carrying out this research. The work was supported by Grants GM-22548 from the National Institutes of Health and CHE-09649 from the National Science Foundation.

APPENDIX

Expressions used for the pseudoatom charge density and its scattering factor are similar to those of Stewart (1976). The charge density of a pseudoatom at a point with spherical coordinates (r, θ, φ) with respect to the atom center is assumed to be

$$\rho(r, \theta, \varphi) = \rho_{\text{core}}(r) + \sum_{l=0}^{L} \sum_{m=0}^{l} C_{lm\pm} R_{nl}(r) Y_{lm\pm}(\theta, \varphi)$$

where $\rho_{\text{core}}(r)$ is a spherical core charge density component which may be derived from self-consistent K-shell wave functions (Clementi, 1965) as in refinements S and SC or from isolated Hartree–Fock atoms in refinement H. The one-electron radial functions are assumed to be of Slater-type with

$$R_{n,l}(r) = \frac{1}{4\pi} \frac{\alpha^{n+3}}{(n+2)!} r^n \exp(-\alpha r)$$

where the integer n has values $n \geq l$. For C, O and N pseudoatoms n was assigned values 2, 2, 2, 3, for monopole, dipole, quadrupole and octapole terms, *i.e.* for $l = 0, 1, 2, 3$ respectively. For H pseudoatoms corresponding values of n were 0, 1, 2 with octapoles neglected. The radial parameter α was assumed to be the same for all pseudoatoms of the same type (C, N or H atoms). In refinements S and SC, α for each atom type was included as a least-squares variable. The angular functions are spherical harmonics, with

$$Y_{lm\pm}(\theta, \varphi) = P_l^m(\cos\theta) \begin{cases} \cos(m_+ \varphi) \\ \sin(m_- \varphi) \end{cases}$$

The least-squares refinement program (Craven & Weber, 1977) provides values of population parameters $C_{lm\pm}$ for angular functions referred to Cartesian crystal axes a, b, c^*. Subsequently, these values may be transformed by rotation to a molecular Cartesian system using the procedure of Cromer, Larson & Stewart (1976). This rotation does not change the form of the angular functions, $Y_{lm\pm}$. Population parameters were also renormalized according to Hansen & Coppens (1978) so as to represent monopole ($l = 0$), dipole ($l = 1$), quadrupole ($l = 2$) and octapole ($l = 3$) charge deformations on a common scale. Normalization factors are obtained by integrating each Y_{lm} over all directions with a common sign. When referred to a Cartesian axial system, the explicit expression for the charge density of a pseudoatom becomes

$$\begin{aligned}
\rho(\mathbf{r}) = \rho_{\text{core}}(r) &+ p_v R_{n,o}(r) \\
&+ 4R_{n,1}(r)[d_1 r_x + d_2 r_y + d_3 r_z] \\
&+ R_{n,2}(r)[4{\cdot}717 q_1(r_x^2 - r_y^2) + 9{\cdot}434 q_2 r_x r_y \\
&+ 9{\cdot}434 q_3 r_x r_z + 9{\cdot}434 q_4 r_y r_z \\
&+ 2{\cdot}598 q_5(3r_z^2 - 1)] \\
&+ R_{n,3}(r)[5{\cdot}319 o_1(r_x^2 - 3r_y^2) r_x \\
&+ 5{\cdot}319 o_2(3r_x^2 - r_y^2) r_y + 12{\cdot}5 o_3(r_x^2 - r_y^2) r_z \\
&+ 25{\cdot}0 o_4 r_x r_y r_z + 4{\cdot}032 o_5(5r_z^2 - 1) r_x \\
&+ 4{\cdot}032 o_6(5r_z^2 - 1) r_y + 3{\cdot}077 o_7(5r_z^2 - 3) r_z]
\end{aligned}$$

where (r_x, r_y, r_z) are direction cosines of $\mathbf{r}$ with respect to the Cartesian axial system and the coefficients $C_{lm\pm}$ are rewritten as p_v, d_j, q_j and o_j for monopoles, dipoles, quadrupoles and octapoles respectively. This is the expression which was used in constructing Figs. 2 and 3, from the values of p_v, d, q and o given in Table 2.

In the least-squares refinement, the corresponding pseudoatom scattering factors were given by

$$f(\mathbf{s}) = \int \rho(\mathbf{r}) \exp(i\mathbf{s}.\mathbf{r})\, d\mathbf{r}$$

which can be expressed as

$$\begin{aligned} f(\mathbf{s}) = {} & f_{\text{core}}(s) + f_v p_v + 4if_d(d_1 s_x + d_2 s_y + d_3 s_z) \\ & + i^2 f_q[4{\cdot}717q_1(s_x^2 - s_y^2) + 9{\cdot}434q_2 s_x s_y \\ & + 9{\cdot}434q_3 s_x s_z + 9{\cdot}434q_4 s_y s_z \\ & + 2{\cdot}598q_5(3s_z^2 - 1)] \\ & + i^3 f_o[5{\cdot}319o_1(s_x^2 - 3s_y^2) s_x \\ & + 5{\cdot}319o_2(3s_x^2 - s_y^2) s_y + 12{\cdot}5o_3(s_x^2 - s_y^2) s_z \\ & + 25{\cdot}0o_4 s_x s_y s_z + 4{\cdot}032o_5(5s_x^2 - 1) s_x \\ & + 4{\cdot}032o_6(5s_z^2 - 1) s_y + 3{\cdot}077o_7(5s_z^2 - 3) s_z] \end{aligned}$$

where $i = \sqrt{-1}$ and (s_x, s_y, s_z) are direction cosines of **s**, the Bragg vector with respect to the same Cartesian axial system used for **r**. Explicit functions for the one-electron radial scattering factors of Slater-type were obtained from equation $A2$ in Epstein & Stewart (1977). They are:

$f_v = (1 + c^2)^{-2}$ for H atoms ($n = 0$), or $(1 - c^2)(1 + c^2)^{-4}$ for C and N atoms ($n = 2$)

$f_d = (5c/3)(1 - c^2/5)(1 + c^2)^{-4}$

$f_q = 2c^2(1 + c^2)^{-4}$

$f_o = (16c^3/5)(1 + c^2)^{-5}$

where $c = (4\pi a_o/\alpha)(\sin\theta/\lambda)$ and $a_o = 0{\cdot}52918$ Å, θ is the Bragg angle, λ is the X-ray wavelength (Å) and α (in atomic units, bohr^{-1}) is the radial parameter for each kind of pseudoatom.

References

BENTLEY, J. & STEWART, R. F. (1975). *J. Chem. Phys.* **63**, 3794–3803.

BLOW, D. M. (1976). *Acc. Chem. Res.* **9**, 145–152.

CLEMENTI, E. (1965). *IBM J. Res. Dev. Suppl.* **9**, 2.

CRAVEN, B. M. & BENCI, P. (1981). *Acta Cryst.* B**37**, 1584–1591.

CRAVEN, B. M., CHANG, C. H. & GHOSH, D. (1979). *Acta Cryst.* B**35**, 2962–2966.

CRAVEN, B. M. & MCMULLAN, R. K. (1979). *Acta Cryst.* B**35**, 934–945.

CRAVEN, B. M., MCMULLAN, R. K., BELL, J. D. & FREEMAN, H. C. (1977). *Acta Cryst.* B**33**, 2585–2589.

CRAVEN, B. M. & WEBER, H.-P. (1977). *The POP Least-Squares Refinement Procedure*, Tech. Rep., Department of Crystallography, Univ. of Pittsburgh.

CROMER, D. T., LARSON, A. C. & STEWART, R. F. (1976). *J. Chem. Phys.* **65**, 336–349.

CROMER, D. T. & WABER, J. T. (1965). *Acta Cryst.* **18**, 104–109.

EPSTEIN, J. (1978). PhD Thesis, Carnegie–Mellon Univ., Pittsburgh, PA 15213.

EPSTEIN, J. & STEWART, R. F. (1977). *J. Chem. Phys.* **66**, 4057–4064.

EPSTEIN, J. & STEWART, R. F. (1979*a*). *J. Chem. Phys.* **70**, 5515–5521.

EPSTEIN, J. & STEWART, R. F. (1979*b*). *Acta Cryst.* A**35**, 476–481.

FOX, R. O., WEBER, H. P. & CRAVEN, B. M. (1982). *Acta Cryst.* Submitted.

HAMILTON, W. C. (1974). *International Tables for X-ray Crystallography*, Vol. IV, pp. 285–310. Birmingham: Kynoch Press.

HANSEN, N. K. & COPPENS, P. (1978). *Acta Cryst.* A**34**, 909–921.

JOHNSON, C. K. & LEVY, H. A. (1974). *International Tables for X-ray Crystallography*, Vol. IV, pp. 311–336. Birmingham: Kynoch Press.

MCMULLAN, R. K., BENCI, P. & CRAVEN, B. M. (1980). *Acta Cryst.* B**36**, 1424–1430.

MCMULLAN, R. K., EPSTEIN, J., RUBLE, J. R. & CRAVEN, B. M. (1979). *Acta Cryst.* B**35**, 688–691.

MARTÍNEZ-CARRERA, S. (1966). *Acta Cryst.* **20**, 783–789.

STEWART, R. F. (1976). *Acta Cryst.* A**32**, 565–574.

STEWART, R. F., DAVIDSON, E. R. & SIMPSON, W. T. (1965). *J. Chem. Phys.* **42**, 3175–3187.

WILL, G. (1969). *Z. Kristallogr.* **129**, 211–221.